CDF note 7792

Measurement of the $t\bar{t}$ production cross section in the missing $\not{E}_T$ + jets channel.

The CDF Collaboration
URL http://www-cdf.fnal.gov

August 25, 2005

Abstract

We present the measurement of the $t\bar{t}$ production cross section in the missing $\not{E}_T$ + jets channel.

We study events collected by a multi-jet trigger and selected using optimized kinematical criteria and containing jets identified in the Silicon VerteX detector as originating from b-quarks.

In this new approach significant missing transverse energy and related geometrical properties, rather than lepton identification requirements, are used to discriminate top quark pair production from background processes. Moreover, parametrized probabilities of b-jet identification, measured directly from data, are used to predict the overall amount of background-produced b-jets in the kinematically selected sample.

Using 311 pb^{-1} of collected data we measure $\sigma_{t\bar{t}} = 5.9 \pm 1.2(stat)^{+1.4}_{-1.0}(syst)pb$.

Preliminary Results for Summer 2005 Conferences

1 Introduction

This note describes a measurement of the $t\bar{t}$ production cross section[1] in $\bar{p}p$ collisions at $\sqrt{s} = 1.96$ TeV with the CDF[2] detector at the Fermilab Tevatron in the missing E_T + jets channel. This channel was not studied previously and the outcoming results add a small piece of knowlegde in the top physics sector.

The signal we are interested in is mainly produced by lepton(e,μ,τ)+jets $t\bar{t}$ decays. Anyway, rather than specific lepton identification based selections, we used significant missing transverse energy and related geometrical properties to discriminate the quark pair production from background pocesses. In order to further enhance the signal over background ratio reached by applying the kinematical selection, we used b-jet identification provided by a secondary vertex tagging algorithm. In particular b-jet identification parametrized probabilities, measured directly from data, are used to predict the overall amount of background-produced b-jets in the kinematically selected sample.

2 Data samples and event prerequisites

This analysis is based on an integrated luminosity of 311 pb^{-1} collected with the CDF detector between March 2002 and August 2004. The data are collected with a multijet trigger that requires at least one calorimetric tower with $E_T \geq 10\ GeV$ at Level 1; at Level 2, at least four clusters wiht $E_T \geq 15\ GeV$ and a total transverse energy exceeding 125 GeV are required. Finally, the third level of the trigger system asks for at least four jets, with $E_T \geq 10\ GeV$.

As far as the Monte Carlo is concerned, it is used for the $t\bar{t}$ samples generation aimed at optimizing the kinematical selection and at determining its efficiency and systematics. In particular, samples generated with $M_{top} = 178\ GeV/c^2$ using PYTHIA and HERWIG, with different ISR/FSR and PDFs tuning have been used for the estimate of the relevant systematic uncertainties. Generated events are reconstructed using a realistic simulation of the CDF detector and trigger system.

2.1 Event prerequisites

In order to have a clean sample of events we applied the following prerequisites:

- We require the events to belong to runs in the good run list defined by the CDF data quality group.
- We reject events with a good, $high-pt$ electron or muon to avoid overlaps with other top lepton+jets analyses.
- We ask for at least one *good quality* vertex with $|z_{vert}| < 60\ cm$.

The number of data events surviving these preliminary requirements is 3,897,755.

N jet	3	4	5	6	7	8
Nevts	879,187	1,553,525	859,543	284,062	68,628	13,237
N tgbl jets	1,781,645	4,197,888	2,877,148	1,134,089	318,410	69,966
Obs + tags	57,314	135,056	87,332	32,914	8,992	1,914
Exp + tags	$57,314 \pm 233$	$133,275 \pm 546$	$87,156 \pm 370$	$33,184 \pm 149$	$9,147 \pm 43$	$2,000 \pm 10$
					Total observed + tags:	323,522
					Total expected + tags:	$322,076 \pm 717$

Table 1: *Tagging matrix check before any kinematical selection. For each jet multiplicity bin, the number of observed and predicted positive tags is shown.*

3 Background prediction

The approach we adopted in order to estimate the background contribution yielded by processes other than $t\bar{t}$ production in the sample with at least one jet identified as originating from a b-quark (*i.e.* with at least one *tagged jet* or *tag*) is here discussed.

The expected amount of background tags is used in order to optimize the kinematical selection, as described in the next section.

We essentially used the rate difference of b-jet identification between $t\bar{t}$ events and all other background processes, that will populate the signal region, to distinguish them. A tagging probability is calculated using 3-jet events collected by the multijet trigger before any kinematical selection, and it is used to predict the amount of background tags in higher jet multiplicity events and in different samples defined by some kinematical selections.

This method rests on the verified assumption that even if the relative contribution from QCD and/or electro-weak proceses changes as a function of the jet multiplicity, the probability for a *taggable* jet (*i.e.* a jet inside the acceptance of the silicon detector) to be tagged (*i.e.* identifiend as originating from a b-quark) remains flat with the jet multiplicity.

In order to track possible sample composition changes introduced by requiring or not a given kinematical cut, the tagging rate, defined by the ratio:

$$\mathcal{P} = \frac{N\ of\ tagged\ jets}{N\ of\ taggable\ jets}$$

is parametrized as a function of the jet E_T, N_{trk} and missing E_T projection along the jet direction.

This kind of parametrization derived from the sample of data with exactly 3-jet events, is used to construct a 3-dimentional matrix able to assign to a jet, given its characteristics, a probability to be identified as a b-jet.

The ability of the matrix in predicting the correct amount of background tagged jet is shown as a function of the jet multiplicity for the sample of data events before any kinematical selection in Tab. 1 and Fig. 1.

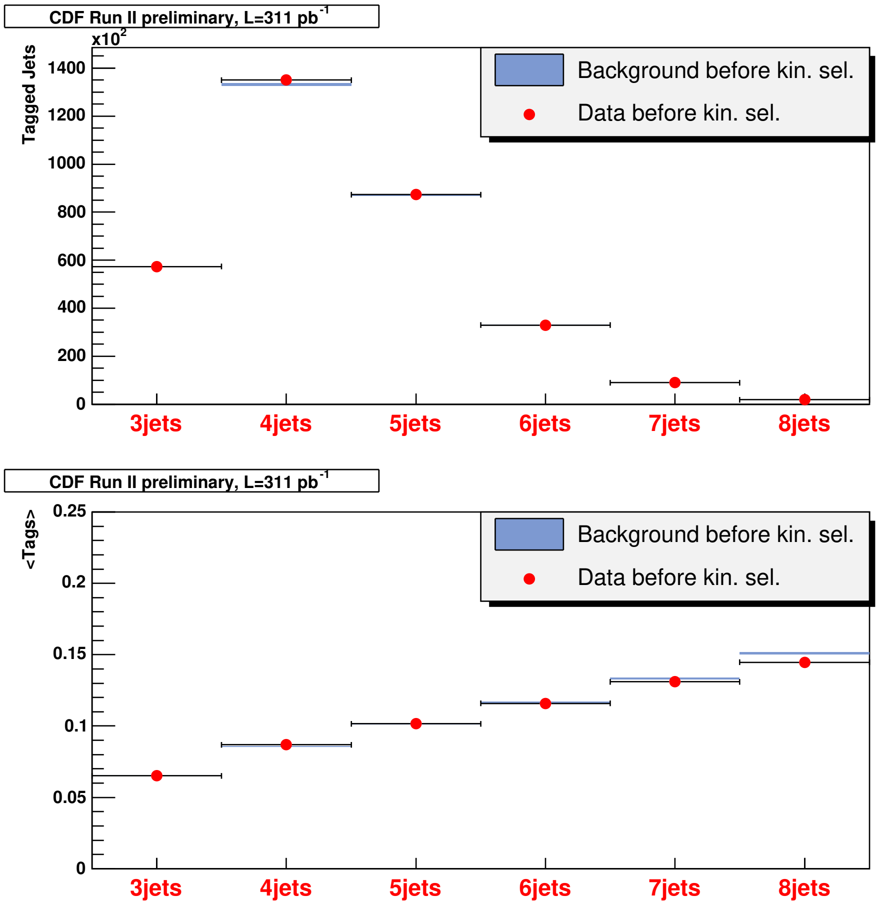

Figure 1: *Tagging matrix check before any kinematical selection. Top plot: observed and predicted positive tags as a function of the jet multiplicity. Bottom plot: average number of observed and predicted tags per event as a function of the jet multiplicity.*

4 Kinematical selection

We set up an optimization procedure in order to choose among different set of cuts on $[\not\!\!E_T/\sqrt{\Sigma E_T},\ A,\ \min\Delta\phi(\not\!\!E_T, jet)]$ the one promising the minimum relative error on a cross section measurement.

Shortly, significant $\not\!\!E_T$ is in general a good indicator for establishing the presence of neutrinos in the event. The missing E_T is correlated with the ΣE_T of the events and, in particular, given that its resolution is shown to degrade as the ΣE_T increases in the form ${\not\!\!E_T}^{res} = const \cdot \sqrt{\Sigma E_T}$, we decided to use the missing E_T significance, defined as $\not\!\!E_T/\sqrt{\Sigma E_T}$, as a selection variable.

On the other hand, aplanarity[1] is in general found to have some discrimination power against the multijet background.

Moreover, the minimum $\Delta\phi$ difference between the $\not{E}_T$ and jet direction was found to provide us with an extra handle in order to further increase the signal to noise ratio in the data we were selecting. While, in fact, for signal events we can expect little correlation between the direction of the given jet and the $\not{E}_T$, the latter quantity being determined by the presence of neutrinos from W decays, on the other hand, as far as the background is concerned we can expect the missing E_T to be mainly due to jet energy mismeasurement and then to be aligned with the jet direction.

The cross section measurement will be given by the following:

$$Xsec = \frac{N^{tag}_{obs} - N^{tag}_{exp}}{\epsilon_{kin} \times \epsilon_{tag} \times \mathcal{L}}$$

where N^{tag}_{obs} and N^{tag}_{exp} are the number of observed and matrix predicted tags respectively, ϵ_{kin} is the efficiency of the kinematical selection on inclusive Monte Carlo $t\bar{t}$ events, ϵ_{tag} is defined as the Monte Carlo ratio between the number of positive tagged jets and the number of events in the pretag sample, and finally $\mathcal{L}$ is the luminosity of the dataset used.

If we use instead of N^{tag}_{obs}, the quantity $N^{tag}_{exp} + N^{tag}_{MC-exp}$, we are able to predict the statistical uncertainty affecting the measurement, before looking at the "post tagging" data sample, and in this way to choose among multiple set of cuts the one that is expected to minimize the relative error on the cross-section measurement.

The list of the analyzed set of cuts was then ordered by increasing relative statistical error on a cross section measurement. Results are reported for the top five selections in Tab. 2. The cross section uncertainty is calculated using only the statistical errors of the involved quantities.

Using the results described above, we chose for our analysis the kinematical selection based on the following analysis cuts:

- $N_{jet}(E^{L5}_T \geq 15\ GeV, |\eta| \leq 2.0) \geq 4$
- $\not{E}_T/\sqrt{\Sigma E_T} \geq 4\ GeV^{1/2}$
- $\min \Delta\phi(\not{E}_T, jets) \geq 0.4\ rad$

which provide an efficiency on signal events of $(4.88 \pm 0.84)\%$ and selecting 597 data events results in a S/N ratio of about 1/5. Finally with these requirements, ϵ_{tag} is found to be $(78.89 \pm 4.58)\%$.

[1] $A = \frac{3}{2}Q_1$ where Q_1 is the smallest of the normalized eigenvalues of the sphericity tensor $M_{ab} = \Sigma_j P^j_a P^j_b$, P^j being the jet four-momentum (aplanarity values range between zero and 0.5; the extreme values are reached in the case of two opposite jets and in the case of evenly distributed jets respectively).

cut set				MC^{evt}_{inc}	MJ^{evt}	MC^{tag}_{inc}	BKG^{tag}	$S/\sqrt{N}$	$\frac{\sigma_{xsec}}{xsec}$
1	4.00	0.00	0.40	93	597	73	67 $\pm$ 3	8.91	17.47%
2	4.00	0.00	0.50	82	461	65	46 $\pm$ 3	9.55	17.48%
3	4.00	0.01	0.40	90	549	71	63 $\pm$ 4	8.93	17.60%
4	4.00	0.01	0.50	80	426	63	43 $\pm$ 3	9.60	17.60%
5	4.00	0.02	0.40	85	494	68	58 $\pm$ 3	8.91	17.84%
...	...	...	...	...	...	...	...	...	...

Table 2: *Different possible kinematical selections ordered by increasing relative error on the cross section measurement, and their figures of merit ($S/\sqrt{N}$ and $\sigma_{xsec}/xsec$), in term of different choices of the cuts for $\not\!\!E_T/\sqrt{\Sigma E_T}$, A, $\Delta\phi_{min}(\not\!\!E_T, jet)$. For each cut set the number of events in the pretag sample and the number of expected tags is shown for Monte Carlo and data respectively. The amount of tags in data are obtained from tagging matrix prediction.*

4.1 Positive tagging matrix predictions in control samples

Once the kinematical selection is defined, we can use its cuts in order to construct control samples close to the signal region and then to use them to further check the tagging matrix predictions, *i.e.* its ability to correctly predict the background contribution in a given sample.

The left panel of Fig. 2 shows how we constructed the control samples:

1) multijet data before any kinematical selection;

2) multijet data with $\not\!\!E_T/\sqrt{\Sigma E_T} \geq 3$ and $\min \Delta\phi(\not\!\!E_T, jet) \leq 0.3$;

3) multijet data with $\not\!\!E_T/\sqrt{\Sigma E_T} \leq 3$ and $\min \Delta\phi(\not\!\!E_T, jet) \geq 0.3$.

The right panel of Fig. 2 on the other hand shows the performance of the tagging matrix in the control sample previously defined in terms of the ratio of observed to matrix-predicted tags.

In the figure, light and dark shaded areas indicate the 5% and 10% discrepancy bands respectively. The overall discrepancy between observed and matrix predicted number of tags can be quoted very conservatively at 10%. The single discrepancy at very high jet multiplicity for control the second control region is not a concern given that our acceptance for 8-jet events is almost null. The 10% discrepancy so calculated will be the systematics amount of uncertainty to be associated to our background prediction.

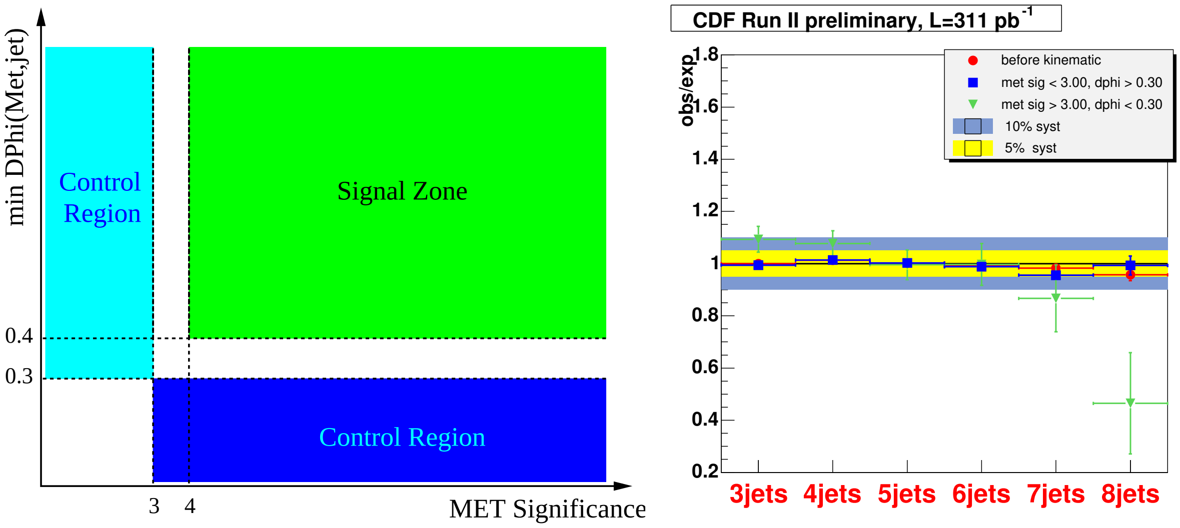

Figure 2: *Left panel: signal and control region definitions in the* $\not\!\!E_T/\sqrt{\Sigma E_T}$, $\min\Delta\phi(\not\!\!E_T, jet)$ *plane. Right panel: observed to matrix predicted positive tagged jets ratio in the control samples : 1) multijet data before any kinematical selection, 2) multijet data with* $\not\!\!E_T/\sqrt{\Sigma E_T} \geq 3$ *and* $\min\Delta\phi(\not\!\!E_T, jet) \leq 0.3$*; 3) multijet data with* $\not\!\!E_T/\sqrt{\Sigma E_T} \leq 3$ *and* $\min\Delta\phi(\not\!\!E_T, jet) \geq 0.3$*. Light and dark shaded areas indicate the 5% and 10% discrepancy bands.*

5 Results

The predicted amount of background after the complete kinematical selection is shown by the grey histograms in Fig. 3[2] together with the theoretically expected $t\bar{t}$ contribution both for the exclusive $\tau + jets$[3] and inclusive channels; the observed positive tags are shown by dots.

In the figure, a good agreement between observed and predicted background tags is observed in the 3 jet bin, where the matrix was computed before the kinematical selection, while on the contrary in the 4 to 6 jet bins we need to add the $t\bar{t}$ Monte Carlo contribution in order to explain the behavior of experimental data.

In order to further establish the $t\bar{t}$ presence in the selected data we performed binned likelihood fits to kinematical distributions of the final data sample. We fitted $\not\!\!E_T$ and $\Delta\phi(\not\!\!E_T, tagged\ jet)$ data distributions (see Fig. 4). The templates used to fit the data were on one hand extracted from the $t\bar{t}$ inclusive Monte Carlo sample, and on the other hand derived from the positive tagging matrix application to data (*i.e.* weigthing each jet in the events with its positive tagging probability returned by the tagging matrix), the latter

[2]In the Figure the expected background contribution is iteratively corrected for the $t\bar{t}$ presence in the pre-tagging sample; see Sec. 7.

[3]The $\tau + jets$ $t\bar{t}$ decay is not observed yet, and this analysis shows large acceptance for these kind of events.

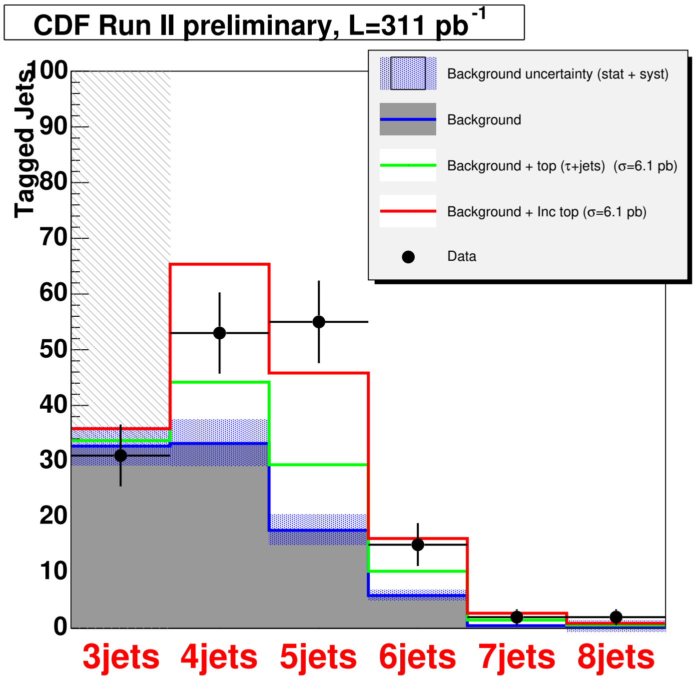

Figure 3: *Tagging matrix background predictions after kinematical selection* $\not\!\!E_T/\sqrt{\Sigma E_T} \geq 4$ *and* $\min \Delta\phi(\not\!\!E_T, jets) \geq 0.4$. *The predicted number of positive tags as a function of the jet multiplicity is shown for background, together with the expected contribution from* $t\bar{t} \to \tau + jets$ *and inclusive Monte Carlo events. Points refers to the observed positive SecVtx tagged jet in the data.*

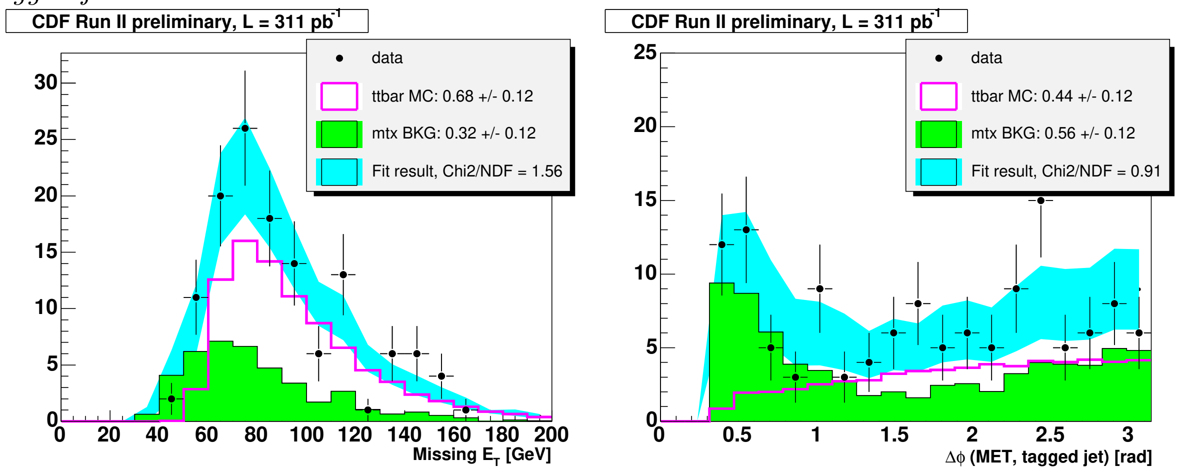

Figure 4: $\not\!\!E_T$ *and* $\Delta\phi(\not\!\!E_T)$ *distributions for data after kinematical selection and with at least one positive SecVtX tag. The distributions are fitted to the sum of Monte Carlo and background templates, the latter being derived from the tagging matrix application to data.*

Systematics uncertainty sources		
Source	Method	Uncertainty
ϵ_{kin} systematics		
Trigger simulation	turn-on curves	14.8 %
Generator dependence	$\frac{\lvert\epsilon_{PYTHIA}-\epsilon_{HERWIG}\rvert}{\epsilon_{PYTHIA}}$	8.2 %
PDFs	MC reweighting	1.6 %
ISR/FSR	samples comparison	2.0 %
Jet Corrections	$\frac{\lvert\epsilon_{jetcorr,+1\sigma}-\epsilon_{jetcorr,-1\sigma}\rvert}{2\epsilon_{kin}}$	1.5 %
ϵ_{tag} systematics		
SecVtX scale factor	$\frac{\lvert\epsilon_{tag,+1\sigma}-\epsilon_{tag,-1\sigma}\rvert}{2\epsilon_{tag}}$	5.8 %
Tagging matrix systematics		
Data control samples	N_{obs}/N_{exp}	10.0 %
Luminosity systematics		
Luminosity measurement	–	6.0 %

Table 3: *Systematics uncertainty sources.*

being intended as background template. Both templates are derived after having applied the kinematical selection; and finally, as far as data and Monte Carlo distributions are concerned, there is an entry per each tagged jet in the event.

In Fig. 4 data distributions are drawn with points, moreover, the fit results and the associated errors are shown by the light shaded areas. The filled histograms represent the background template; the $t\bar{t}$ contribution is represented by the open histogram and both the templates are normalized to the values returned by the fits.

The $t\bar{t}$ component in the selected data extracted by means of the fits is in agreement with the overall prediction of the tagging matrix in the N_{jet} spectrum (Fig. 3).

6 Systematics

The summary of all the systematic uncertainty sources is listed in Tab. 3.

7 Cross section

After the application of the kinematical selection we are left with 597 data events for $4 \leq N_{jet} \leq 8$, out of which 106 have at least one b-tagged jet, for a total of 127 tags.

The expected number of tags provided by the positive tagging matrix parametrization is $N_{exp}^{tags} = 67.4 \pm 2.7(stat) \pm 6.7(syts) = 67.4 \pm 7.2$. Anyway, the expectation does not

N evt	$MC_{(\tau+jets)}$	$MC_{Incl.}$	MJ
Total	149,323	1,021,924	4,249,644
Prereq	74,904	558,528	3,897,755
$N_{jet} \geq 4$	72,708	549,138	2,781,788
$\not{E}_T/\sqrt{\Sigma E_T} \geq 4$	29,830	78,145	3,996
$\min \Delta\phi(\not{E}_T, jets) \geq 0.4$	19,079	49,848	597
≥ 1 tag	11,666	30,410	106
in 311 pb^{-1}:	21.7	56.5	106
S/N $\tau + jets$: $N^{\tau}_{mc}/(N^{data}_{obs} - N^{incl}_{mc})$			0.44
S/N Inclusive: $N^{incl}_{mc}/(N^{data}_{obs} - N^{incl}_{mc})$			1.14

Table 4: *Effect of the kinematical selection $N_{jet}(E_T^{L5} \geq 15, |\eta| \leq 2.0) \geq 4$, $\not{E}_T/\sqrt{\Sigma E_T} \geq 4$, $\min \Delta\phi(\not{E}_T, jets) \geq 0.4$ and ≥ 1 SecVtx positive tag on $t\bar{t} \to \tau + jets$ and $t\bar{t}$ inclusive events as well as on multijet data sample. The row named as Prereq contains the clean up+trigger requirements.*

Variable	Simbol	Input Value	Output Value
Integrated Luminosity (pb^{-1})	$\mathcal{L}$	311 ± 18	311 ± 18
Observed Tags	N_{obs}	127	$-$
Expected Tags	N'_{exp}	57.4 ± 8.1	57.0 ± 8.1
Kin efficiency (%)	ϵ_{kin}	4.878 ± 0.838	4.813 ± 0.854
Ave Tag efficiency (%)	ϵ_{tag}	78.89 ± 4.58	78.74 ± 4.58

Table 5: *Input and output values of the likelihood maximization.*

refer to background events only, since it receives a small contribution from $t\bar{t}$ events in the pre-tagging sample. The consequence of this is that we need to remove the $t\bar{t}$ contribution in order to have a background-only contribution in the number of expected tags. To do so, we iteratively correct the number of expected tags as follows

$$N'_{exp} = N^{fix}_{exp} \frac{N_{evt} - N^{t\bar{t}}_{evt}}{N_{evt}} = N^{fix}_{exp} \frac{N_{evt} - \frac{N_{obs} - N_{exp}}{\epsilon^{ave}_{tag}}}{N_{evt}}$$

the procedure stops when the difference $|N'_{exp} - N_{exp}| \leq 1\%$. The results of this approach is that 10.0 out of 67.4 tags are attributed to the $t\bar{t}$ presence in the pre-tagging sample yielding a top-free background determination of $N'_{exp} = 57.4 \pm 8.1$.

The excess of tags defined as $N_{obs} - N'_{exp}$ is associated to the $t\bar{t}$ production and used for the cross section measurement.

The cross section is measured by maximizing $\log \mathcal{L}$, where the likelihood function is defined as follows:

$$
\mathcal{L} = e^{-\frac{(L-\bar{L})^2}{2\sigma_L^2}} \cdot e^{-\frac{(\epsilon_{kin}-\bar{\epsilon}_{kin})^2}{2\sigma_{\epsilon_{kin}}^2}} \cdot e^{-\frac{(\epsilon_{tag}-\bar{\epsilon}_{tag})^2}{2\sigma_{\epsilon_{tag}}^2}} \cdot e^{-\frac{(N'_{exp}-\bar{N}'_{exp})^2}{2\sigma_{N'_{exp}}^2}} \cdot
\cdot \frac{(\sigma_{t\bar{t}} \cdot \epsilon_{kin} \cdot \epsilon_{tag} \cdot L + N'_{exp})^{N_{obs}}}{N_{obs}!} \cdot e^{-(\sigma_{t\bar{t}} \cdot \epsilon_{kin} \cdot \epsilon_{tag} \cdot L + N'_{exp})}
$$

The central value is given by the likelihood maximization, that is:

$$
\sigma_{t\bar{t}} = \frac{N_{obs} - N'_{exp}}{\epsilon_{kin} \cdot \epsilon_{tag} \cdot L}.
$$

The input and output parameters of the likelihood maximization are quoted in Tab.5 The measured cross section value is found to be:

$$
\sigma_{t\bar{t}} = 5.9 \pm 1.2(stat) \ {}^{+1.4}_{-1.0}(syst) \quad pb = 5.9 \ {}^{+1.8}_{-1.6} \quad pb.
$$

Fig. 5 the number of expected and observed tags as a function of the jet multiplicity together with the expectation from Monte Carlo $t\bar{t}$ events are presented for the measured cross section value of 5.9 pb.

The acceptance calculation for the results here provided assumes a $M_{top} = 178\ GeV/c^2$, the value currently published as world average. The dependence of the measured cross section on the input top mass is shown in Fig. 6 together with the theoretical expectations.

8 Conclusions

In order to isolate the $t\bar{t} \to \not{E}_T + jets$ signal in the data collected with a multijet trigger, we set up our analysis constructing a positive tagging matrix, in which the background tagging rate was parametrized as a function of jet E_T, N_{trk} and ${\not{E}_T}^{prj} = \not{E}_T \cos\Delta\phi(\not{E}_T, jet)$. The performance of the matrix and in particular its capability to correctly predict the amount of background tags were checked in control samples depleted of signal contamination. The discrepancy between observed and predicted tags was found to be limited at 10% level.

Using the tagging matrix prediction we optimized the kinematical selection by minimizing the relative statistical error on a cross section measurement. The best choice of cuts was found to be: $N_{jet}(E_T^{L5} \geq 15\ GeV, |\eta| < 2.0) \geq 4$, $\not{E}_T/\sqrt{\Sigma E_T} \geq 4.0$ and $\min \Delta\phi(\not{E}_T, jet) \geq 0.4$. With these requirements we ended up in the pre-tagging sample with 93 events expected from $t\bar{t}$ inclusive events against 597 observed events in the multijet data sample. This selection provided us with a signal over background ratio of 0.18.

The final sample to be used for a cross section measurement was finally defined by means of the additional requirement of at least one b-tagged jet; in this sample the signal to background ratio was found to be 1.14, being 56.5 the number of inclusive $t\bar{t}$ events expected in 311 pb^{-1} of multijet data respectively, out of 106 observed events.

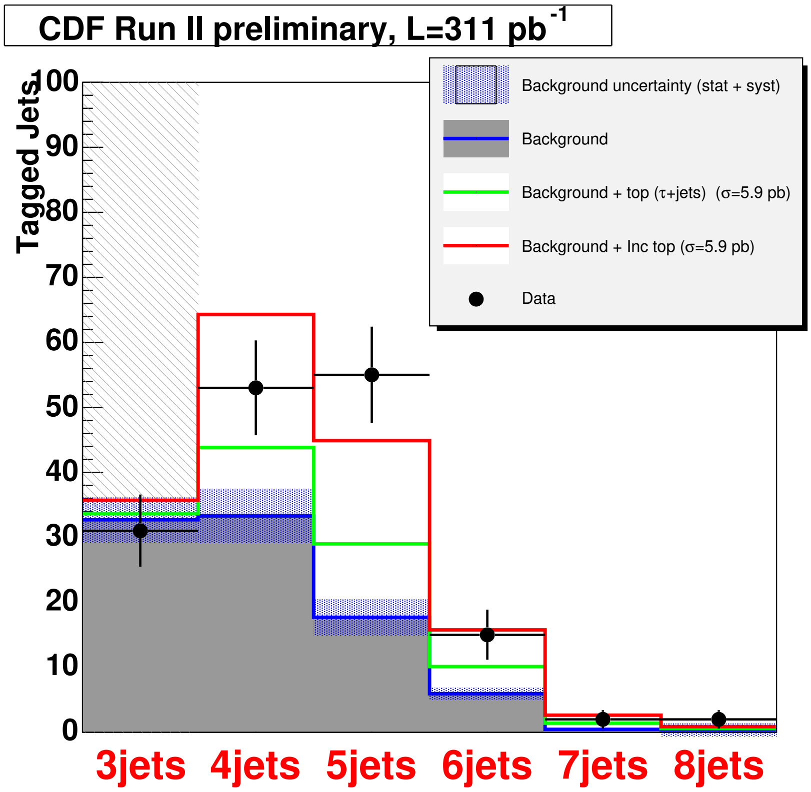

Figure 5: *Number of tagged jet versus jet multiplicity. Data (points), background iteratively corrected (shaded histogram) and $t\bar{t}$ expectation (lines) ($\sigma_{t\bar{t}} = 5.9$ pb) are shown after kinematical selection.*

Moreover, the inclusive $t\bar{t}$ contribution in the final sample was cross-checked by means of two-component fits to kinematical distributions of tagged data. The observed spectra were indeed fit to the sum of Monte Carlo $t\bar{t}$ inclusive and background templates, the latter being the results of the matrix application in the sample of data after kinematical selection.

With all these ingredients we were able to measure a $t\bar{t}$ cross section of
$\sigma_{t\bar{t}} = 5.9 \pm 1.2(stat)\ ^{+1.4}_{-1.0}(syst)\ \ pb = 5.9\ ^{+1.8}_{-1.6}\ \ pb.$

9 Acknowledgments

We thank the Fermilab staff and the technical staffs of the participating institutions for their vital contributions. This work was supported by the U.S. Department of Energy and National Science Foundation; the Italian Istituto Nazionale di Fisica Nucleare; the Ministry of Education, Culture, Sports, Science and Technology of Japan; the Natural Sciences and Engineering Research Council of Canada; the National Science Council of

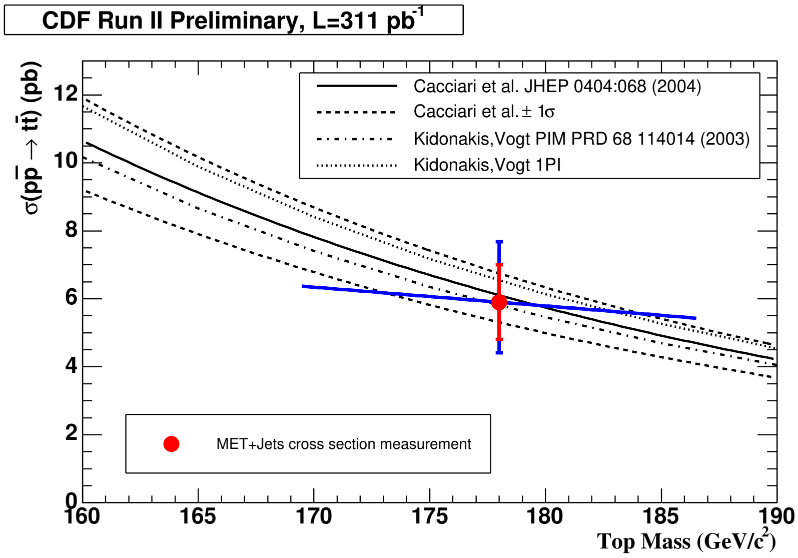

Figure 6: *$t\bar{t}$ cross section as a function of M_{top}. The point with error bar corresponds to the measured cross section $\sigma_{t\bar{t}} = 5.9\ ^{+1.8}_{-1.6}$ pb. The measurement is compared to the theory predictions.*

the Republic of China; the Swiss National Science Foundation; the A.P. Sloan Foundation; the Bundesministerium fuer Bildung und Forschung, Germany; the Korean Science and Engineering Foundation and the Korean Research Foundation; the Particle Physics and Astronomy Research Council and the Royal Society, UK; the Russian Foundation for Basic Research; the Comision Interministerial de Ciencia y Tecnologia, Spain; and in part by the European Community's Human Potential Programme under contract HPRN-CT-20002, Probe for New Physics.

References

[1] M. Cacciari *et al.*, The $t\bar{t}$ Cross-section at 1.8 TeV and 1.96 TeV: A Study of the Systematics due to Parton Densities and Scale Dependence, JHEP **404**, 68 (2004).

[2] F. Abe *et al.*, Nucl. Instrum. Methods Phys. Res. A **271**, 387 (1988); D. Amidei *et al.*, Nucl. Instum. Methods Phys. Res. A **350**, 73 (1994); F. Abe *et al.*, Phys. Rev. D **52**, 4784 (1995); P. Azzi *et al.*, Nucl. Instrum. Methods Phys. Res. A **360**, 137 (1995); The CDFII Detector Technical Design Report, Fermilab-Pub-96/390-E